Chem

CellPress

Article

Superhydrophobicity: Constructing Homogeneous Catalysts into Superhydrophobic Porous Frameworks to Protect Them from Hydrolytic Degradation

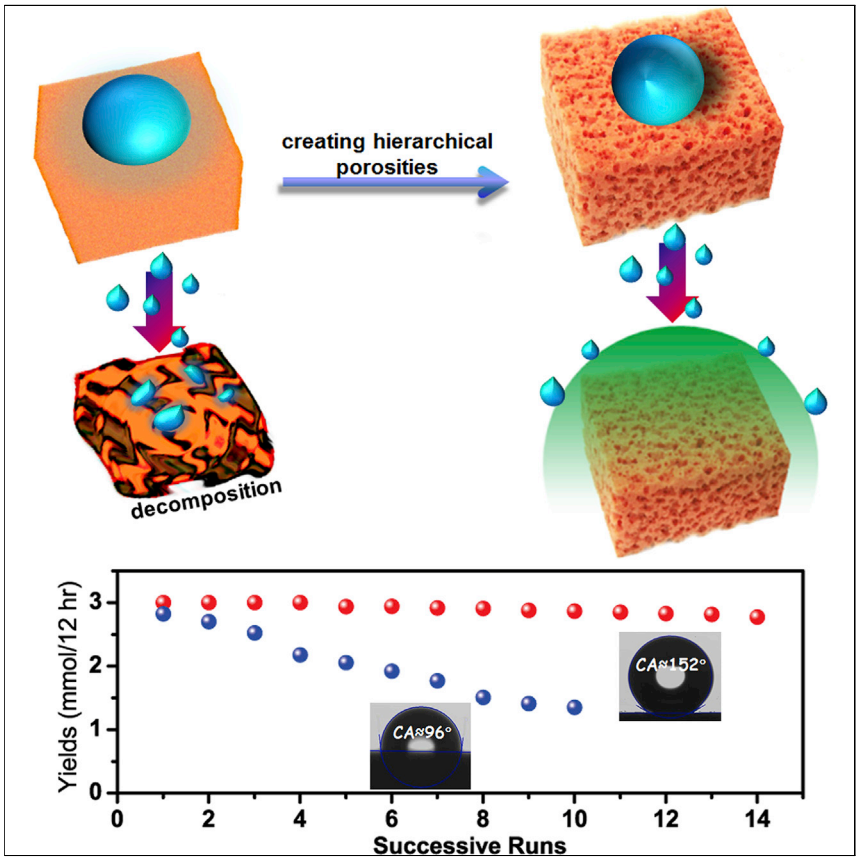

Resistance against hydrolytic degradation of water-sensitive homogeneous catalysts can be dramatically boosted by the formation of superhydrophobic porous frameworks. Compared with their homogenous counterparts, the resultant catalysts exhibit superior performance and can be readily recycled for reuse without loss of performance. The approach advanced in this work is extendable, thereby providing a new perspective for protecting catalyst materials from hydrolysis issues.

Qi Sun, Briana Aguila, Gaurav Verma, ..., Xiangju Meng, Feng-Shou Xiao, Shengqian Ma

fsxiao@zju.edu.cn (F.-S.X.)
sqma@usf.edu (S.M.)

HIGHLIGHTS

Realizing superhydrophobicity for catalysts by introducing hierarchical porosity

Boosted water tolerance of catalysts via construction into superhydrophobic polymers

Superior catalytic performances after formation of superhydrophobic porous frameworks

Sun et al., Chem 1, 628–639
October 13, 2016 © 2016 Elsevier Inc.
http://dx.doi.org/10.1016/j.chempr.2016.09.008

Chem

CellPress

Article

Superhydrophobicity: Constructing Homogeneous Catalysts into Superhydrophobic Porous Frameworks to Protect Them from Hydrolytic Degradation

Qi Sun,[1,2] Briana Aguila,[2] Gaurav Verma,[2] Xiaolong Liu,[3] Zhifeng Dai,[1] Feng Deng,[3] Xiangju Meng,[1] Feng-Shou Xiao,[1,*] and Shengqian Ma[2,4,*]

SUMMARY

Hydrolytic degradation has caused numerous efficient catalytic systems to suffer because in many cases it is impossible to fully exclude water from the reaction systems. Here, we demonstrate an effective strategy of stabilizing water-sensitive organic-ligand-based homogeneous catalysts by constructing them into a superhydrophobic porous framework, which renders them extraordinarily water resistant yet fully retains their intrinsic catalytic activities under heterogeneous systems. Representatively, after metalation of the superhydrophobic porous phosphite-ligand-based framework with Rh species, the resultant catalyst exhibits superior activities and dramatically enhanced durability in mimic continuous hydroformylation processes of the internal olefins in comparison with the homogeneous counterparts. In addition, because it is solid in nature, the catalyst can be readily recycled with negligible loss of performance. Given the modular nature and the broad scope of organic ligands, our work opens a new avenue for stabilizing water-sensitive homogeneous catalysts into highly water-tolerate heterogeneous catalysts.

INTRODUCTION

Engineering the wettability of solid materials has attracted tremendous interest from researchers because of their versatile potential for application in a broad range of fields.[1–7] Control of the wettability of a catalyst surface is widely known to be of great importance for enhancing catalytic performance.[8–12] For example, hydrophobic catalysts have a unique repellency for water, resulting in increased activity as well as prevention of water-induced poisoning of active sites in various reactions involving water as a byproduct.[13–15] In this context, we envision that imparting superhydrophobicity (superhydrophobic materials have a contact angle exceeding 150° for a water droplet) on water-sensitive catalysts may provide a unique opportunity to protect them against hydrolytic degradation, which has caused problems in a number of efficient catalytic systems because in many cases it is impossible to fully exclude water from the reaction systems.[16,17] Nevertheless, studies on hydrophobic engineering to address catalyst hydrolysis issues have rarely been explored.

Recently, porous organic polymers (POPs) have been established as a highly designable platform for developing advanced materials because of the tunability of porous structures and the flexibility of molecular design.[18–30] Various organic compounds have been successfully transformed into superhydrophobic polymers via the introduction of hierarchically porous structures during the polymerization process.[31–34] For example,

The Bigger Picture

Nature utilizes the extreme water-repellent properties of superhydrophobic surfaces to protect living things from water permeation. To mimic biological functions, anti-wetting artificial materials with features such as self-cleaning and anti-fogging have garnered widespread applications. Hydrolysis is a reaction involving the breaking of a bond in a molecule by water. A number of catalysts suffer from inherent hydrolysis problems, and in many cases it is impossible to fully exclude water from reaction systems. Here, by virtue of the unique water repellency of superhydrophobic materials, we contribute an effective approach for boosting the durability of water-sensitive ligands against hydrolysis via the construction of superhydrophobic porous polymers. The results are of great importance because the catalysts are well protected and maintain high catalytic activities, thereby providing a new perspective for enhancing the water resistance of catalysts.

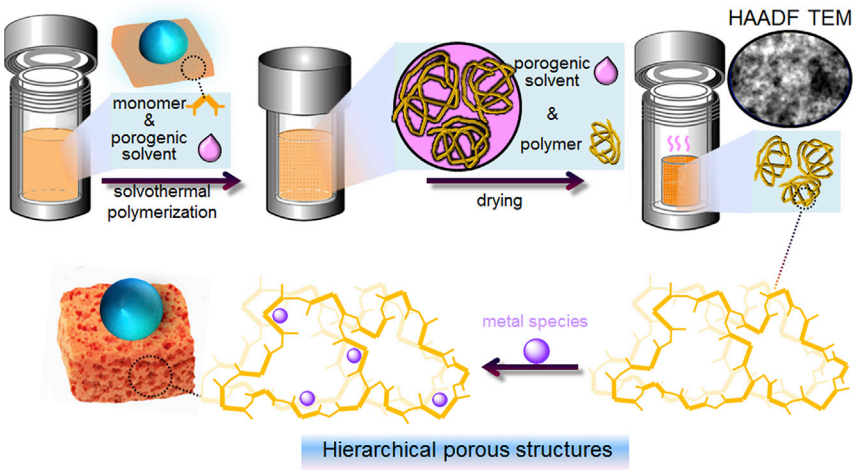

Figure 1. Illustration of the Synthesis of Superhydrophobic POP Loaded with Metal Species
See also Figure S1.

polymerization of vinyl-functionalized monomers in the presence of suitable porogenic solvents has been proven to be a powerful strategy for fabricating hierarchically porous polymers with potential superhydrophobic properties.[35,36] This strategy is anticipated to realize the hydrophobic requirement of catalysts and does not introduce new constituents or more complex chemical modifications that may result in the loss of catalytic activity. Bearing the above considerations in mind, we reason that if water-sensitive organic ligand-based homogeneous catalysts can be polymerized into superhydrophobic porous framework, then the resulting POPs with enhanced hydrophobicity can not only circumvent the issue of hydrolysis but also inherit the advantages of heterogeneous catalysts, such as ease of recovery.[37,38]

Here, we contribute a general and effective approach for boosting the durability of water-sensitive organic ligands against hydrolysis via the construction of a superhydrophobic porous organic polymer framework (Figure 1). Phosphite ligands were chosen to demonstrate the proof of concept, because these types of ligands can be readily metalated to serve as efficient catalysts for various reactions (e.g., hydroformylation of internal olefins).[39–42] However, they possess relatively low water tolerance because the P–O bonds are inclined to hydrolyze.[42] Through rational design of the vinyl-functionalized phosphite monomers and careful adjustment of the porogenic solvents, we successfully polymerized the phosphite ligand to form a hierarchically porous structure, which renders the polymer with bulk superhydrophobicity (hereafter denoted as phosphite-POP). The hierarchically porous structure also made the phosphite coordination sites highly accessible, which was subsequently post-synthetically metalated with Rh species to afford the catalyst (hereafter denoted as Rh/phosphite-POP). The resultant catalyst has excellent catalytic activities and extraordinary durability in the context of hydroformylation of internal olefins, even in the presence of water. This work presents a promising example of stabilizing moisture-sensitive ligands via the construction of a superhydrophobic porous framework, thereby providing a new perspective on enhancing the water resistance of catalysts.

RESULTS

Synthesis of Superhydrophobic POPs

As a representative sample of synthesized superhydrophobic POPs based on phosphite ligands (Figure S1), the preparation of the POP constructed by

[1]Key Lab of Applied Chemistry of Zhejiang Province, Department of Chemistry, Zhejiang University, Hangzhou 310028, China

[2]Department of Chemistry, University of South Florida, 4202 East Fowler Avenue, Tampa, FL 33620, USA

[3]State Key Laboratory of Magnetic Resonance and Atomic and Molecular Physics, Wuhan Institute of Physics and Mathematics, Chinese Academy of Sciences, Wuhan 430071, China

[4]Lead Contact

*Correspondence: fsxiao@zju.edu.cn (F.-S.X.), sqma@usf.edu (S.M.)

http://dx.doi.org/10.1016/j.chempr.2016.09.008

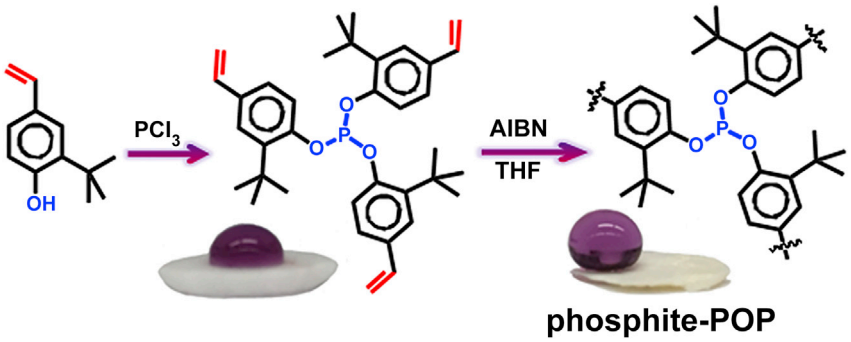

Figure 2. Synthetic Route of Phosphite-POP and Corresponding Photos of Water Droplets on the Pellet Disk Made from the Monomer and the Polymer

Water droplets: 0.24 wt % Arsenazo III solution. See also Figures S2–S4.

tris(2-*tert*-butylphenyl) phosphite is described in detail. As shown in Figure 2, the tris(2-*tert*-butyl-4-vinylphenyl) phosphite monomer was achieved by treatment of 2-*tert*-butyl-4-vinylphenol with PCl_3. Phosphite-POP was obtained in near 100% yield by polymerization of the monomer under solvothermal conditions in tetrahydrofuran (THF) at 100°C for 24 hr in the presence of azobisisobutyronitrile (AIBN). Solvent test results revealed that the polymers synthesized in this work were insoluble in water and common organic solvents such as DMSO, dimethylformamide (DMF), THF, and $CHCl_3$.

Structure Characterization of Phosphite-POP

The local chemical structure of the resultant phosphite-POP was characterized by ^{13}C magic-angle spinning (MAS) nuclear magnetic resonance (NMR) and ^{31}P MAS NMR spectroscopy studies (Figures S2–S4), which indicated that the tris(2-*tert*-butyl-4-vinylphenyl) phosphite moieties were stable during the polymerization process.

The surface morphology of phosphite-POP was examined by scanning electron microscopy (SEM; Figure 3A). Interestingly, phosphite-POP displayed a rough surface with abundant pores from several nanometers to over tens of nanometers. The sample roughness is expected to be very beneficial to enhance the sample hydrophobicity according to the "lotus effect."[1–6] The transmission electron microscopy (TEM) image of phosphite-POP (Figure 3B) clearly demonstrates the hierarchically porous structures in the framework.

The hierarchical porosity of phosphite-POP was further confirmed by its nitrogen sorption isotherms at 77 K (Figure 3C). It exhibited a sharp uptake of N_2 at low relative pressure ($P/P_0 < 0.1$) and a hysteresis loop at higher relative pressure ($0.4 < P/P_0 < 0.8$), indicating the existence of both micro- and mesopores in the framework. Analysis of pore-size distribution calculated by the nonlocal density functional theory (NLDFT) indicated that its pore sizes were predominantly distributed around 0.5–1.4 and 2–10 nm (Figure S5). Derived from the N_2 adsorption data, the BET (Brunauer-Emmett-Teller) surface area and pore volume of phosphite-POP were estimated to be 643 m^2/g and 0.43 cm^3/g, respectively.

Wettability Test of Phosphite-POP

The superhydrophobicity of phosphite-POP has been demonstrated from the contact angle of a water droplet on its surface, which can be as high as 152°

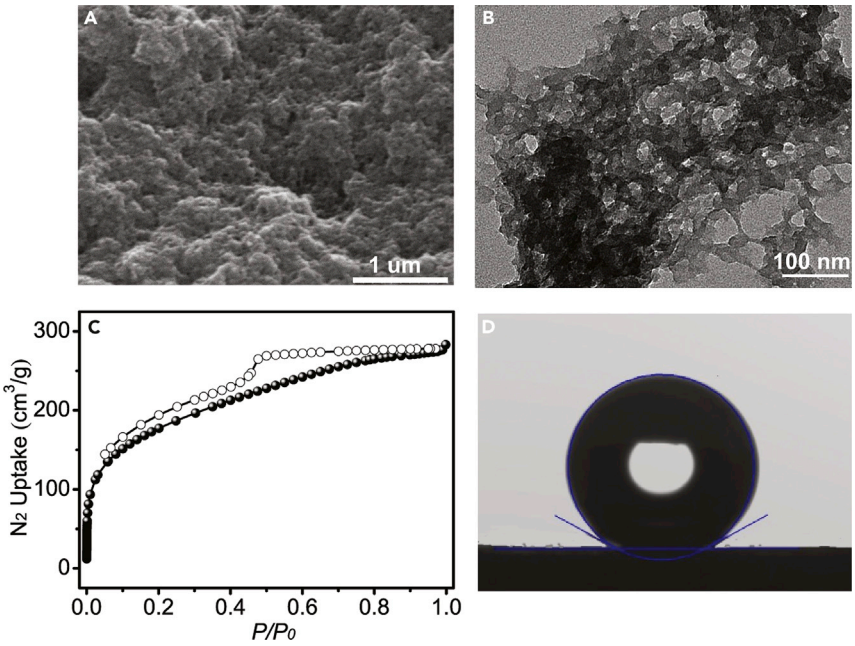

Figure 3. Characterization of Phosphite-POP

SEM image (A), TEM image (B), N_2 sorption isotherms (C), and photograph (D) of a water droplet on the pellet disk made from phosphite-POP. Scale bars represent 1 μm (A) and 100 nm (B). See also Figures S5–S9.

(Figure 3D). In contrast, the soluble phosphite ligand tris(2-*tert*-butylphenyl) phosphite affords a contact angle of water of 96° (Figure S6A); the polymeric phosphite ligand without hierarchically porous structures (hereafter denoted as poly-phosphite), which was synthesized with acetone as the polymerization solvent, showed a contact angle of water of 110° (Figure S6B). Considering that phosphite-POP and poly-phosphite have almost the same chemical composition, the superhydrophobicity observed for phosphite-POP should stem from its hierarchically porous structure. Water-vapor sorption isotherms revealed that phosphite-POP exhibits a negligible water uptake capacity even at P/P_0 up to 0.9, indicating that the superhydrophobicity can effectively prevent water molecules from entering its pores (Figure S7).[43]

Hydrolytic Stability Test of Phosphite-POP

It has been documented that aryl phosphites are inclined to decompose through hydrolysis of P–O bonds to form phenols.[42] This presents a major hurdle for their application as catalysts when metalated with metal ions, given that water is inevitably involved either as a byproduct or as an impurity in many important reactions in industry. Therefore, in order to maintain the long-term high activity of phosphite-based catalysts, it is essential that their water resistance be enhanced. We first examined the water stability of tris(2-*tert*-butylphenyl) phosphite and phosphite-POP. The two phosphite materials were refluxed by a deliberately wet toluene solvent (5.0 wt % water), and the degree of hydrolysis for each sample was monitored by ^{31}P-NMR spectroscopy. It was observed that the superhydrophobic phosphite-POP fully retained its phosphite moieties (Figure S8A) and hierarchically porous structure (Figure S8B) even after a 10-day treatment, indicating its excellent water resistance. In contrast, hydrolysis occurred within 12 hr for tris(2-*tert*-butylphenyl) phosphite (Figure S9), ~57% of the phosphite was

Table 1. Catalytic Data in the Hydroformylation of 2-Octene over Various Catalysts

Entry	Catalyst	Yield (%)[a]	Select (%)[b]
1	Rh/phosphite-POP	>99.5	>99.5
2[c]	Rh/phosphite-tBu	95.5	>99.5
3	Rh/poly-phosphite	67.2	>99.5

Reaction conditions: 2-octene (3.0 mmol), toluene (10 mL), 100°C, 12 hr, catalyst based on Rh (0.033 mol %), and CO/H_2 = 1:1 (2.0 MPa).
[a]Aldehyde yield.
[b]Aldehyde selectivity.
[c]The mole ratio of tris(2-*tert*-butylphenyl) phosphite to Rh was 9. See also Tables S1–S3.

decomposed after 2 days, and complete hydrolysis of tris(2-*tert*-butylphenyl) phosphite was observed in 5 days. These results highlight that the superhydrophobicity of phosphite-POP renders it with the ability to protect phosphite moieties against hydrolysis.

Encouraged by the above results, we treated phosphite-POP with $[Rh(acac)(CO)_2]$ (acac = acetylacetonate) to afford Rh/phosphite-POP (2.0 wt % loading of Rh) and investigated the catalysis performance of Rh/phosphite-POP in the context of hydroformylation of olefins to aldehydes, which is one of the most important chemical processes in industry[44–46] but involves the inevitable generation of water because of condensation of aldol from aldehyde products.[42] Control catalysis experiments were also conducted for Rh-metalated tris(2-*tert*-butylphenyl) phosphite (hereafter denoted Rh/phosphite-tBu) and poly-phosphite (2.0 wt % loading of Rh, hereafter denoted as Rh/poly-phosphite).

Synthesis and Characterization of Rh/Phosphite-POP

The hierarchically porous structure of phosphite-POP was preserved after metalation with 2.0 wt % Rh, as indicated by the SEM and TEM images (Figure S10) and N_2 sorption isotherms at 77 K (Figure S11). Meanwhile, Rh/phosphite-POP inherited the superhydrophobicity, as demonstrated by a water contact angle of 151° (Figure S10B, inset). The X-ray photoelectron spectroscopy (XPS) spectrum of Rh/phosphite-POP demonstrates the binding energies of $Rh3d_{5/2}$ and $Rh3d_{3/2}$ at 308.5 and 313.2 eV, respectively, which are lower than those of $Rh(CO)_2(acac)$ (309.9 and 314.6 eV). Meanwhile, the P2d binding energy of Rh/phosphite-POP (133.5 eV) is higher than that of the parent phosphite-POP (133.1 eV) (Figure S12). These results suggest that strong interactions exist between the Rh and tris(2-*tert*-butylphenyl) phosphite moieties in the phosphite-POP.[47]

Evaluation of Catalytic Performance and Long-Term Stability

Given increasing interest in the production of nonanol as an alternative plasticizer alcohol,[48] we chose 2-octene as a model substrate to evaluate the performance of various internal olefins, which currently remain a challenge in the chemical industry.[49–51] Table 1 presents catalytic data for the hydroformylation of 2-octene over heterogeneous catalysts of Rh/phosphite-POP and Rh/poly-phosphite (Rh loading was optimized at 2.0 wt %, where the ligand/Rh molar ratio was ~9; Figure S13) as well as the homogeneous catalysts of Rh/phosphite-tBu. Notably, Rh/phosphite-POP afforded a very high 2-octene conversion (>99.5%) and aldehyde selectivity (>99.5%) after 12 hr. When the homogeneous counterpart of the Rh/phosphite-tBu was used, the conversion (95.5%) was slightly lower than that of Rh/phosphite-POP (Figure 4A), indicating that the activity of the phosphite ligand can be fully retained when constructed into a hierarchical porous structure (Table S1). The slightly accelerated reaction rate observed for Rh/phosphite-POP

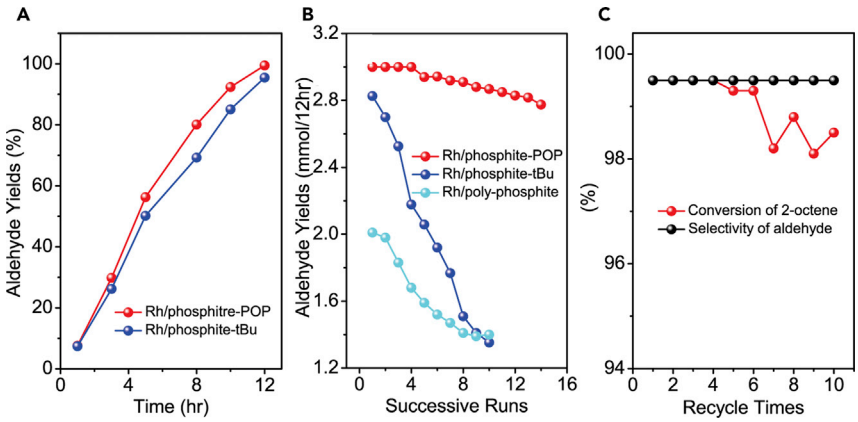

Figure 4. Catalytic Kinetics, Long-Term Stability Tests, and Recyclability Tests

(A) Plots of aldehyde yields versus time of 2-octene hydroformylation.

(B) Long-term stability in 2-octene hydroformylation operated in a deliberately wet toluene solvent (5.0 wt % H_2O); the L/Rh ratio in Rh/phosphite-tBu was 9.

(C) Recycling tests for Rh/phosphite-POP. Reaction conditions: 2-octene (3.0 mmol), solvent (10 mL), 100°C, 12 hr, catalyst based on Rh (0.033 mol %), and CO/H_2 = 1:1 (2.0 MPa).

See also Figures S10–S15.

in comparison with the homogeneous counterpart can presumably be attributed to enrichment of the reactants within the nanopores.[52] The benefit of the porous structure in Rh/phosphite-POP for catalysis is further highlighted by the fact that the nonporous Rh/poly-phosphite (Rh loading at 2.0 wt %) exhibited a much lower conversion of 67.2%.

For examination of the durability of Rh/phosphite-POP, Rh/phosphite-tBu, and Rh/poly-phosphite under the reaction conditions with a small amount of water, mimic continuous hydroformylation processes were performed in deliberately wet toluene solvent (5.0 wt % H_2O) with consecutive introduction of substrate and gases every 12 hr. The plots of aldehyde yields with an interval of 12 hr (mmol/12 hr) versus each successive run of 2-octene hydroformylation catalyzed by Rh/phosphite-POP, Rh/phosphite-tBu, and Rh/poly-phosphite are displayed in Figure 4B. It is noteworthy that Rh/phosphite-POP maintained its high catalytic performance with just a slight loss of activity after 14 successive runs over a period of 1 week (3.0 mmol/12 hr for the first run versus 2.77 mmol/12 hr for the 14^{th}), highlighting its excellent durability. This is in striking contrast with its homogeneous counterpart, Rh/phosphite-tBu, which experienced a steady decrease in catalytic activity, such that the yield dramatically reduced to 1.35 mmol/12 hr at the tenth run. In addition, a consistently high aldehyde selectivity (>99.5%) was observed for Rh/phosphite-POP over the 1 week reaction period, whereas a certain amount of paraffin byproduct was detected in the reaction system catalyzed by Rh/phosphite-tBu at the third run (ca. 0.033 mmol/12 hr), and the amount increased to 0.192 mmol/12 hr at the tenth run. With regard to Rh/poly-phosphite, it started to lose its activity from the third run and exhibited a steady decline in yield from 2.01 mmol/12 hr at the first run to 1.40 mmol/12 hr at the tenth run. We reason that the observed decrease in both activities and selectivities for Rh/phosphite-tBu and Rh/poly-phosphite should be attributed to the hydrolysis of the phosphite ligand, as suggested from the aforementioned studies on the water stability of tris(2-*tert*-butylphenyl) phosphite. In contrast, the superhydrophobicity of Rh/phosphite-POP can effectively repel water molecules to prevent hydrolysis of the phosphite moieties, thereby preserving the high activity and

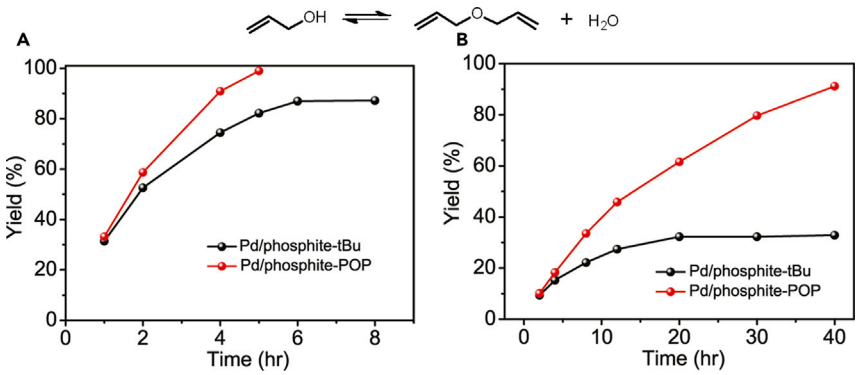

Figure 5. Catalytic Kinetics and Durability Tests in the Reactions Involving Water as a Byproduct
Plots of 3-(allyloxy)prop-1-ene yield (%) versus time for Pd-catalyzed dehydrative allylation of 2-propene-1-ol using Pd/phosphite-tBu and Rh/phosphite-POP as catalysts. Reaction conditions: (A) 2-propene-1-ol (10 mmol), Pd catalyst (0.5 mol %), and 80°C under a N_2 atmosphere; (B) 2-propene-1-ol (50 mmol), Pd catalyst (0.1 mol %), and 80°C under a N_2 atmosphere. See also Figure S21.

high selectivity of the catalyst over a long period of reaction time. These inferences have been verified by the ^{31}P-NMR analysis (Figures S14 and S15).

No detectable leaching of Rh species was found in the supernatant of the reaction system catalyzed by Rh/phosphite-POP, which can be readily recycled with negligible loss of its catalytic performance in terms of both activity and selectivity (Figure 4C), highlighting its heterogeneous nature. Notably, the hierarchical porous structure of Rh/phosphite-POP was fully retained after a long period of use (ten times; Figure S16). The scope of Rh/phosphite-POP as a heterogeneous catalyst for the hydroformylation of internal olefins has also been studied on the basis of various aliphatic, aromatic, and heteroatom-substituted internal olefins as substrates, all of which were hydroformylated in high yields (>99.5%; Table S2), highlighting the broad applicability of such catalytic systems.

To verify the applicability of the strategy in the reaction involving water as a byproduct, Pd-catalyzed dehydrative allylation of 2-propene-1-ol reactions were studied. The time course of the conversion of 2-propene-1-ol into 3-(allyloxy)prop-1-ene in the presence of an optimized ratio of homogeneous tris(2-*tert*-butylphenyl) phosphite (2 mol %) and $Pd_2(dba)_3$ (0.25 mol %) at 80°C indicated that the product yield reached ca. 87% after 6 hr. However, no further conversion was obtained even after prolonged reaction time (Figure 5A), suggesting that 2-propene-1-ol should be in equilibrium with product and water under the reaction conditions. Impressively, when Pd/phosphite-POP (phosphite/Pd around 4) synthesized by treatment of $Pd_2(dba)_3$ and phosphite-POP was used, the product yield was higher than 99.0% within 5 hr, which suggests that the reaction equilibrium was disturbed and shifted to the positive side after the water molecules formed in situ were quickly excluded from the catalyst.

To support the low water retention of Pd/phosphite-POP, thereby enhancing the durability of the catalyst, we compared the activities of Pd/phosphite-POP and Pd/phosphite-tBu at low catalyst loading (0.1 mol %). Time-dependent conversion curves indicated that the reaction catalyzed by Pd/phosphite-POP was much faster than that catalyzed by the homogeneous Pd/phosphite-tBu. The yield steadily increased over time in the presence of Pd/phosphite-POP. In striking contrast,

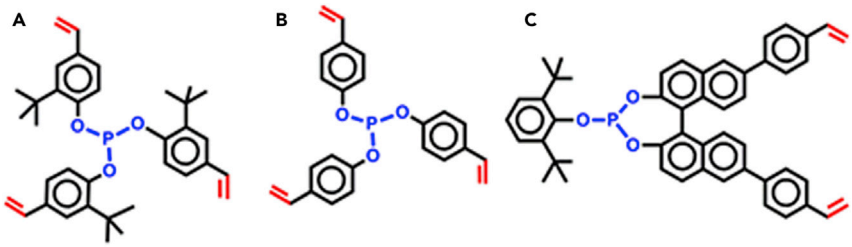

Figure 6. Structures of Vinyl-Functionalized Phosphite Ligands
Phosphite-POP (A), H-phosphite-POP (B), and BINOL-phosphite-POP (C). See also Figures S16–S25.

Pd/phosphite-tBu was deactivated after 20 hr, and prolonging the reaction time did not lead to any additional product formation (Figure 5B).

DISCUSSION

In summary, we have demonstrated an effective strategy for enhancing the durability of water-sensitive homogeneous catalysts via the formation of a superhydrophobic porous framework, as illustrated by the construction of a hierarchically porous phosphite-based framework. The superhydrophobicity, stemming mainly from the hierarchically porous structure, provides the catalyst with superior activity and excellent durability in comparison with the homogeneous counterpart, as exemplified in the context of catalytic hydroformylation of internal olefins. Moreover, this strategy can be readily extended to other phosphite ligands (Figures 6 and S17–S25 and Tables 2 and S3), and significantly enhanced durability in relation to the homogeneous control was observed. For instance, Pd/H-phosphite was deactivated within 8 hr in the dehydrative allylation of 2-propene-1-ol, as demonstrated by the negligible increase in product yield, whereas Pd/H-phosphite-POP remained active for even 40 hr, giving a product yield as high as 84.5% (Figure S21). Considering the modular nature and the broad scope of organic ligands, our work therefore provides a new way to stabilize water-sensitive homogeneous catalysts into highly durable heterogeneous catalysts. Ongoing work in our laboratories includes investigation of catalysis performance of superhydrophobic POPs based on other phosphite ligands, and the results will be reported separately in due course.

EXPERIMENTAL PROCEDURES

Materials

Solvents were purified according to standard laboratory methods. THF was distilled over $LiAlH_4$. DMF, CH_2Cl_2, and triethylamine were distilled over CaH_2. Other commercially available reagents were purchased in high purity and used without further purification.

Synthesis of Phosphite-POP

As a typical run, 1.0 g of tris(2-*tert*-butyl-4-vinylphenyl) phosphite was dissolved in 20 mL of THF, followed by the addition of 50 mg of AIBN. The mixture was transferred into an autoclave at 100°C for 24 hr. The title polymer was obtained after being washed with CH_2Cl_2 and evaporated under a vacuum.

Synthesis of Rh/Phosphite-POP Catalyst

As a typical synthesis recipe, 0.1 g of the phosphite-POP was swollen in 40 mL of toluene for 30 min, followed by the addition of 5.1 mg of $Rh(CO)_2(acac)$. After being stirred at room temperature under a N_2 atmosphere for 24 hr, the mixture was

Table 2. Structures of Vinyl-Functionalized Phosphite Monomers and Textural Parameters of the Corresponding Porous Polymers

Monomer[a]	Polymer	BET (m^2/g)	Pore Volume (cm^3/g)	Contact Angle (°)
A	phosphite-POP	643	0.43	152
B	H-phosphite-POP	811	0.70	151
C	BINOL-phosphite-POP	523	0.96	155

[a]The structures of the monomers are shown in Figure 6. See also Figures S17–S25 and Table S3.

filtered and washed with excess toluene and finally dried at 50°C under a vacuum. The light-yellow solid obtained was denoted as Rh/phosphite-POP. The combined toluene filtrate was evaporated under a vacuum, and aqua regia (1 mL) was added to dissolve any possible Rh species. Then, the resultant aqua regia was diluted into 10 mL for inductively coupled plasma optical emission spectroscopy (ICP-OES) tests. ICP-OES results revealed that the Rh concentration was below the detection limit (<0.1 ppm), so the Rh loading amount in the phosphite-POP was 2.0 wt %.

Water-Resistance Tests

0.1 g of tris(2-*tert*-butylphenyl) phosphite or phosphite-POP and 10 mL of deliberately wet toluene solvent (5.0 wt % water) were added to a 50 mL Schlenk tube, and the mixture was heated to reflux at different time intervals.

Catalytic Tests

Hydroformylation of Olefins

Rh-based catalyst, internal olefin (3 mmol), and toluene (10 mL) were added to a stainless steel autoclave (100 mL) with a magnetic stir bar. After the mixture was sealed and purged with syngas (CO/H_2 = 1:1) three times, the pressure of syngas was adjusted to the desired value. Then, the autoclave was put into a preheated oil bath with stirring at 100°C for 12 hr at a speed of 1,000 rpm. After the reaction, the catalysts were removed from the system by centrifugation and analyzed by gas chromatography (Kexiao Co. GC-1690 equipped with a flame ionization detector and a Supelco γ-DEX 225 capillary column).

For each recycling, the catalysts were separated by centrifugation under N_2, washed with degassed toluene, and used directly for the next run.

Mimic Continuous Hydroformylation Processes

Rh-based catalysts, 2-octene (3 mmol), and deliberately wet toluene solvent (10 mL, 5.0 wt % H_2O) were added to a stainless steel autoclave (100 mL). After the mixture was sealed and purged with syngas (CO/H_2 = 1:1) three times, the pressure of syngas was adjusted to the desired value. Then, the autoclave was put into a preheated oil bath with stirring at 100°C for 12 hr. After 12 hr, the reaction system was cooled down to room temperature, and the reaction pressure was reduced to atmospheric pressure. Then, a new portion of the substrate and gases were introduced, followed by hydroformylation at 100°C.

Pd-Catalyzed Dehydrative Allylation of 2-Propene-1-ol

In a typical run, Pd/phosphite-POP catalyst (116.5 mg) and 2-propene-1-ol (10 mmol) were added to a Schlenk tube (25 mL) with a magnetic stir bar under a N_2 atmosphere. Then, the Schlenk tube was put into a preheated oil bath with stirring at 80°C. At appropriate time intervals, very small portions of the mixture were removed and diluted with $CDCl_3$, and the catalysts were separated by syringe filter (0.45 μm membrane filter) before analysis by ^{1}H-NMR. With respect to the

homogeneous control (Pd/phosphite-tBu), phosphite-tBu (95.6 mg) and $Pd_2(dba)_3$ (22.9 mg) were used as catalysts. Other procedures were similar, except Pd/phosphite-POP was used as the catalyst. For the catalyst durability tests, 100 mmol of 2-propene-1-ol was used; others were the same as the kinetic experiment.

Characterization

Nitrogen sorption isotherms at −196°C were measured with a Micromeritics ASAP 2020M and Tristar system. The samples were outgassed for 10 hr at 100°C before the measurements. SEM imaging was performed with a Hitachi SU 1510 and SU 4800. TEM imaging was performed with a Hitachi HT-7700 or JEM-2100F field emission electron microscope (JEOL) with an acceleration voltage of 110 kV. XPS spectra were obtained on a Thermo ESCALAB 250 with Al Kα irradiation at $\theta = 90^\circ$ for X-ray sources, and the binding energies were calibrated with the C1s peak at 284.9 eV. ICP-OES analysis was measured with a PerkinElmer Plasma 40 emission spectrometer. ^{1}H-NMR spectra were recorded on a Bruker Avance-400 (400 MHz) spectrometer. Chemical shifts are expressed in ppm downfield from tetramethylsilane at $\delta = 0$ ppm, and *J* values are given in Hertz. ^{13}C (100.5 MHz) cross-polarization (CP)-MAS and ^{31}P (161.8 MHz) MAS NMR experiments were recorded on a Bruker Avance 500 spectrometer equipped with a magic-angle spin probe in a 4-mm (^{13}C) or 1.9-mm (^{31}P) ZrO_2 rotor. Contact angles of water and organic compounds were measured on a contact-angle measuring system (SL200KB, USA KNO Industry Co.) equipped with a CCD camera. The static contact angles were measured in sessile drop mode. Water adsorption and desorption isotherms were obtained with the SMS Instruments DVS Advantage. The balance had a sensitivity of 0.1 μg. Measurement of these isotherms consisted of monitoring the weight change of the sample as a function of the relative humidity of water at 25°C. The relative humidity of water was stepped up from 0% to 98% with an increment of 10% at each step and then stepped down to 0%. Real-time weight, temperature, and relative humidity were recorded.

SUPPLEMENTAL INFORMATION

Supplemental Information includes Supplemental Experimental Procedures, 25 figures, and 3 tables and can be found with this article online at http://dx.doi.org/10.1016/j.chempr.2016.09.008.

AUTHOR CONTRIBUTIONS

Q.S., S.M., and F.-S.X. conceived and designed the research. Q.S., S.M., B.A., G.V., X.M., and F.-S.X. drafted the manuscript. Q.S. and Z.D. carried out the synthesis. X.L. and F.D. contributed to NMR characterization of the materials. All authors discussed the results and approved the final version of the manuscript.

ACKNOWLEDGMENTS

The authors acknowledge the University of South Florida, National Natural Science Foundation of China (21273197, 21333009, and 21422306), and National High-Tech Research and Development program of China (2013AA065301) for financial support of this work.

Received: July 14, 2016
Revised: August 15, 2016
Accepted: September 16, 2016
Published: October 13, 2016

REFERENCES AND NOTES

1. Yao, X., Song, Y., and Jiang, L. (2011). Applications of bio-inspired special wettable surfaces. Adv. Mater. *23*, 719–734.

2. Su, B., Tian, Y., and Jiang, L. (2016). Bioinspired interfaces with superwettability: from materials to chemistry. J. Am. Chem. Soc. *138*, 1727–1748.

3. Tian, X., Shaw, S., Lind, K.R., and Cademartiri, L. (2016). Thermal processing of silicones for green, scalable, and healable superhydrophobic coatings. Adv. Mater. *28*, 3677–3682.

4. Bellanger, H., Darmanin, T., de Givenchy, E.T., and Guittard, F. (2014). Chemical and physical pathways for the preparation of superoleophobic surfaces and related wetting theories. Chem. Rev. *114*, 2694–2716.

5. Tuteja, A., Choi, W., Ma, M., Mabry, J.M., Mazzella, S.A., Rutledge, G.C., McKinley, G.H., and Cohen, R.E. (2007). Designing superoleophobic surfaces. Science *318*, 1618–1622.

6. Carné-Sánchez, A., Stylianou, K.C., Carbonell, C., Naderi, M., Imaz, I., and Maspoch, D. (2015). Protecting metal-organic framework crystals from hydrolytic degradation by spray-dry encapsulating them into polystyrene microspheres. Adv. Mater. *27*, 869–873.

7. Zhang, W., Hu, Y., Ge, J., Jiang, H.-L., and Yu, S.-H. (2014). A facile and general coating approach to moisture/water-resistant metal-organic frameworks with intact porosity. J. Am. Chem. Soc. *136*, 16978–16981.

8. Huang, G., Yang, Q., Xu, Q., Yu, S.-H., and Jiang, H.-L. (2016). Polydimethylsiloxane coating for a palladium/MOF composite: highly improved catalytic performance by surface hydrophobization. Angew. Chem. Int. Ed. Engl. *55*, 7379–7383.

9. Dai, Y., Liu, S., and Zheng, N. (2014). C_2H_2 treatment as a facile method to boost the catalysis of Pd nanoparticulate catalysts. J. Am. Chem. Soc. *136*, 5583–5586.

10. Wang, M., Wang, F., Ma, J., Chen, C., Shi, S., and Xu, J. (2013). Insights into support wettability in tuning catalytic performance in the oxidation of aliphatic alcohols to acids. Chem. Commun. *49*, 6623–6625.

11. Liu, F., Wang, L., Sun, Q., Zhu, L., Meng, X., and Xiao, F.-S. (2012). Transesterification catalyzed by ionic liquids on superhydrophobic mesoporous polymers: heterogeneous catalysts that are faster than homogeneous catalysts. J. Am. Chem. Soc. *134*, 16948–16950.

12. Crossley, S., Faria, J., Shen, M., and Resasco, D.E. (2010). Solid nanoparticles that catalyze biofuel upgrade reactions at the water/oil interface. Science *327*, 68–72.

13. Okuhara, T. (2002). Water-tolerant solid acid catalysts. Chem. Rev. *102*, 3641–3666.

14. Yuan, C., Luo, W., Zhong, L., Deng, H., Liu, J., Xu, Y., and Dai, L. (2011). Gold@ polymer nanostructures with tunable permeability shells for selective catalysis. Angew. Chem. Int. Ed. Engl. *50*, 3155–3159.

15. Liu, F., Kong, W., Qi, C., Zhu, L., and Xiao, F.-S. (2012). Design and synthesis of mesoporous polymer-based solid acid catalysts with excellent hydrophobicity and extraordinary catalytic activity. ACS Catal. *2*, 565–572.

16. Verspui, G., Schanssema, F., and Sheldon, R.A. (2000). A Stable, conspicuously active, water-soluble Pd catalyst for the alternating copolymerization of ethene and CO in Water. Angew. Chem. Int. Ed. Engl. *39*, 804–806.

17. Corma, A., Domine, M.E., and Valencia, S. (2003). Water-resistant solid Lewis acid catalysts: Meerwein-Ponndorf-Verley and Oppenauer reactions catalyzed by tin-beta zeolite. J. Catal. *215*, 294–304.

18. Zhang, P., Li, H., Veith, G.M., and Dai, S. (2015). Soluble porous coordination polymers by mechanochemistry: from metal-containing films/membranes to active catalysts for aerobic oxidation. Adv. Mater. *27*, 234–239.

19. Yue, Y., Mayes, R.T., Kim, J., Fulvio, P.F., Sun, X.-G., Tsouris, C., Chen, J., Brown, S., and Dai, S. (2013). Seawater uranium sorbents: preparation from a mesoporous copolymer initiator by atom-transfer radical polymerization. Angew. Chem. Int. Ed. Engl. *52*, 13458–13462.

20. Sun, L.-B., Liu, X.-Q., and Zhou, H.-C. (2015). Design and fabrication of mesoporous heterogeneous basic catalysts. Chem. Soc. Rev. *44*, 5092–5147.

21. Alsbaiee, A., Smith, B.J., Xiao, L., Ling, Y., Helbling, D.E., and Dichtel, W.R. (2016). Rapid removal of organic micropollutants from water by a porous β-cyclodextrin polymer. Nature *529*, 190–194.

22. Du, Y., Yang, H., Whiteley, J.M., Wan, S., Jin, Y., Lee, S.-H., and Zhang, W. (2016). Ionic covalent organic frameworks with spiroborate linkage. Angew. Chem. Int. Ed. Engl. *55*, 1737–1741.

23. Zeng, Y., Zou, R., and Zhao, Y. (2016). Covalent organic frameworks for CO_2 capture. Adv. Mater. *28*, 2855–2873.

24. Fischer, S., Schmidt, J., Strauch, P., and Thomas, A. (2013). An anionic microporous polymer network prepared by the polymerization of weakly coordinating anions. Angew. Chem. Int. Ed. Engl. *52*, 12174–12178.

25. Lin, Q., Bu, X., Kong, A., Mao, C., Bu, F., and Feng, P. (2015). Heterometal-embedded organic conjugate frameworks from alternating monomeric iron and cobalt metalloporphyrins and their application in design of porous carbon catalysts. Adv. Mater. *27*, 3431–3436.

26. Zhuang, X., Gehrig, D., Forler, N., Liang, H., Wagner, M., Hansen, M.R., Laquai, F., Zhang, F., and Feng, X. (2015). Conjugated microporous polymers with dimensionality-controlled heterostructures for green energy devices. Adv. Mater. *27*, 3789–3796.

27. Xiang, Z., Cao, D., Huang, L., Shui, J., Wang, M., and Dai, L. (2014). Nitrogen-doped holey graphitic carbon from 2D covalent organic polymers for oxygen reduction. Adv. Mater. *26*, 3315–3320.

28. Li, B., Guan, Z., Wang, W., Yang, X., Hu, J., Tan, B., and Li, T. (2014). Highly dispersed Pd catalyst locked in knitting aryl network polymers for Suzuki-Miyaura coupling reactions of aryl chlorides in aqueous media. Adv. Mater. *26*, 3315–3320.

29. Slater, A.G., and Cooper, A.I. (2015). Function-led design of new porous materials. Science *348*, 988–998.

30. Feng, X., Chen, L., Honsho, Y., Saengsawang, O., Liu, L., Wang, L., Saeki, A., Irle, S., Seki, S., Dong, Y., and Jiang, D. (2012). An ambipolar conducting covalent organic framework with self-sorted and periodic electron donor-acceptor ordering. Adv. Mater. *24*, 3026–3031.

31. Erbil, H.Y., Demirel, A.L., Avci, Y., and Mert, O. (2003). Transformation of a simple plastic into a superhydrophobic surface. Science *299*, 1377–1380.

32. Genzer, J., and Efimenko, K. (2000). Creating long-lived superhydrophobic polymer surfaces through mechanically assembled monolayers. Science *290*, 2130.

33. Lee, Y., Park, S.-H., Kim, K.-B., and Lee, J.-K. (2007). Fabrication of hierarchical structures on a polymer surface to mimic natural superhydrophobic surfaces. Adv. Mater. *19*, 2330–2335.

34. Li, A., Sun, H.-X., Tan, D.-Z., Fan, W.-J., Wen, S.-H., Qing, X.-J., Li, G.-X., Li, S.-Y., and Deng, W.-Q. (2011). Superhydrophobic conjugated microporous polymers for separation and adsorption. Energy Environ. Sci. *4*, 2062–2065.

35. Levkin, P.A., Svec, F., and Fréchet, J.M.J. (2009). Porous polymer coatings: a versatile approach to superhydrophobic surfaces. Adv. Funct. Mater. *19*, 1993–1998.

36. Zhang, Y., Wei, S., Liu, F., Du, Y., Liu, S., Ji, Y., Yokoi, T., Tatsumi, T., and Xiao, F.-S. (2009). Superhydrophobic nanoporous polymers as efficient adsorbents for organic compounds. Nano Today *4*, 135–142.

37. Fang, Q., Gu, S., Zheng, J., Zhuang, Z., Qiu, S., and Yan, Y. (2014). 3D microporous base-functionalized covalent organic frameworks for size-selective catalysis. Angew. Chem. Int. Ed. Engl. *53*, 2878–2882.

38. Thacker, N.C., Lin, Z., Zhang, T., Gilhula, J.C., Abney, C.W., and Lin, W. (2016). Robust and porous β-diketiminate-functionalized metal-organic frameworks for earth-abundant-metal-catalyzed C-H amination and hydrogenation. J. Am. Chem. Soc. *138*, 3501–3509.

39. Selent, D., Hess, D., Wiese, K.-D., Röttger, D., Kunze, C., and Börner, A. (2001). New phosphorus ligands for the rhodium-catalyzed isomerization/hydroformylation of internal octenes. Angew. Chem. Int. Ed. Engl. *40*, 1696–1698.

40. Seayad, A., Ahmed, M., Klein, H., Jackstell, R., Gross, T., and Beller, M. (2002). Internal olefins to linear amines. Science *297*, 1676–1678.

41. Webb, P.B., Sellin, M.F., Kunene, T.E., Williamson, S., Slawin, A.M.Z., and Cole-Hamilton, D.J. (2003). Continuous flow hydroformylation of alkenes in supercritical fluid-ionic liquid biphasic systems. J. Am. Chem. Soc. *125*, 15577–15588.

42. van Leeuwen, P.W.N.M., and Chadwick, J.C. (2011). Homogeneous Catalysts: Activity-Stability-Deactivation (Wiley VCH), pp. 23–26.

43. Serre, C. (2012). Superhydrophobicity in highly fluorinated porous metal-organic frameworks. Angew. Chem. Int. Ed. Engl. *51*, 6048–6051.

44. Sun, Q., Jiang, M., Shen, Z., Jin, Y., Pan, S., Wang, L., Meng, X., Chen, W., Ding, Y., Li, J., and Xiao, F.-S. (2014). Porous organic ligands (POLs) for synthesizing highly efficient heterogeneous catalysts. Chem. Commun. *50*, 11844–11847.

45. Li, C., Xiong, K., Yan, L., Jiang, M., Song, X., Wang, T., Chen, X., Zhan, Z., and Ding, Y. (2015). Designing highly efficient Rh/CPOL-bp&PPh_3 heterogeneous catalysts for hydroformylation of internal and terminal olefins. Catal. Sci. Technol. *6*, 2143–2149.

46. Li, C., Yan, L., Lu, L., Xiong, K., Wang, W., Jiang, M., Liu, J., Song, X., Zhan, Z., Jiang, Z., and Ding, Y. (2016). Single atom dispersed Rh-biphephos&PPh_3@porous organic copolymers : highly efficient catalysts for continuous fixed-bed hydroformylation of propene. Green. Chem. *18*, 2995–3005.

47. Sun, Q., Dai, Z., Liu, X., Sheng, N., Deng, F., Meng, X., and Xiao, F.-S. (2015). Highly efficient heterogeneous hydroformylation over Rh-metalated porous organic polymers: synergistic effect of high ligand concentration and flexible framework. J. Am. Chem. Soc. *137*, 5204–5209.

48. Selent, D., Wiese, K.-D., Röttger, D., and Börner, A. (2000). Novel oxyfunctionalized phosphonite ligands for the hydroformylation of isomeric *n*-olefins. Angew. Chem. Int. Ed. Engl. *39*, 1639–1641.

49. Yan, Y., Zhang, X., and Zhang, X. (2006). A tetraphosphorus ligand for highly regioselective isomerization-hydroformylation of internal olefins. J. Am. Chem. Soc. *128*, 16058–16061.

50. van der Veen, L.A., Kamer, P.C.J., and van Leeuwen, P.W.N.M. (1999). Hydroformylation of internal olefins to linear aldehydes with novel rhodium catalysts. Angew. Chem. Int. Ed. Engl. *38*, 336–338.

51. Wu, L., Fleischer, I., Jackstell, R., Profir, I., Franke, R., and Beller, M. (2013). Ruthenium-catalyzed hydroformylation/reduction of olefins to alcohols: extending the scope to internal alkenes. J. Am. Chem. Soc. *135*, 14306–14312.

52. Chen, Z., Guan, Z., Li, M., Yang, Q., and Li, C. (2011). Enhancement of the performance of a platinum nanocatalyst confined within carbon nanotubes for asymmetric hydrogenation. Angew. Chem. Int. Ed. Engl. *50*, 4913–4917.